Effect of Water Vapor on Ozone-Induced Lean Methane Oxidation Using Cobalt-Exchanged BEA Catalysts

So Min Jin and Dae-Won Lee[†]

Department of Chemical Engineering, Kangwon National University, 1 Kangwondaehak-gil,
Chuncheon-si, Gangwon-do, 24341, Korea

Abstract – In response to the threats of global warming and climate change, the development of highly energy-efficient lean methane oxidation processes has become crucial. One promising technology is ozone-induced lean methane oxidation (O_3-LMO), which utilizes ozone as an oxidant and a transition metal-loaded zeolite as a catalyst. Our previous study demonstrated that the O_3-LMO system, employing a cobalt-exchanged BEA (Co-BEA) catalyst, effectively abates lean methane (500 ppm) at low temperatures below 200°C under dry conditions. In this study, we investigated the effect of water vapors on the performance of Co-BEA-based O_3-LMO system. The results indicated that CH_4 conversion, CO_2 selectivity, and O_3 utilization efficiency of the system were not significantly affected by water vapors. Additionally, any temporary suppression of activity could be easily reversed through simple vacuum drying of the catalyst. The system maintained robust activity for over 18 hours during prolonged testing under wet conditions.

Key words: Methane abatement, Lean methane oxidation, Ozone, Co-BEA catalyst, Wet activity

1. Introduction

Methane is the second most potent anthropogenic greenhouse gas, following carbon dioxide. Its global warming potential is 28–36 times that of carbon dioxide, meaning that 1 ton of methane absorbs 28–36 times more radiative energy than 1 ton of carbon dioxide [1]. The atmospheric concentration of methane has more than doubled since preindustrial times, reaching approximately 1860 ppb in recent years, significantly contributing to global warming and climate change [2]. The primary sources of anthropogenic methane emissions include fossil fuel extraction and processing, natural gas engine emissions, waste management (landfill gas), and agricultural emissions. Addressing methane emissions is urgent because it accounts for a substantial portion of the total radiative forcing contributing to global warming. Recent estimates indicate that methane's cumulative radiative forcing is 0.62 W·m^{-2}, compared to 1.95 W·m^{-2} for CO_2, from 1755 to 2015 [3].

Given the significant impact of methane on the climate change, there is a pressing need to develop effective strategies for its removal from the atmosphere. Catalytic oxidation is a promising approach, as it can convert methane into less radiation-absorbing carbon dioxide. While complete methane oxidation would slightly increase CO_2 levels, it could reduce about one-sixth of the total radiative forcing of the atmosphere [2]. It is claimed that the catalytic oxidation technologies could restore atmospheric methane concentrations to pre-industrial levels,

providing more time to adapt to warming from carbon dioxide [2].

However, catalytic oxidations using molecular oxygen usually requires reaction temperatures higher than 300℃ [4–6], posing challenges in terms of energy efficiency and additional carbon footprint. Moreover, lean methane oxidation, which oxidizes methane contained in gases with a methane concentration of less than 1%, is especially difficult to implement because it has the kinetic limitations due to low concentration and temperature.

A viable alternative is ozone-induced lean methane oxidation (O_3-LMO), which uses ozone as an oxidant for catalytic lean methane oxidation [4,7-9]. Ozone is a very strong oxidant that can be effectively generated by treating oxygen or air with a non-thermal plasma reactor. It is known that O_3-LMO using transition metal (Co, Fe, or Pd)-loaded zeolite can oxidize lean methane at temperatures lower than 300℃ [4,7,8].

In our previous study, we introduced cobalt-exchanged BEA zeolite (Co-BEA) for its strong O_3-LMO activity in abating the flows containing very low concentration of methane (500 ppm) [4]. However, the study focused on demonstrating the high activity of the Co-BEA catalyst and elucidating the mechanism of its catalysis based on reaction tests using dry reaction gas. In this study, we investigated the performance of Co-BEA-based O_3-LMO system under wet reaction gas conditions and the impact of water vapor on the long-time performance of the system.

2. Experimental

2-1. Preparation of catalyst

Initially, NH₄-BEA zeolite (Si/Al = 12.5, Alfa Aesar) was transformed

[†] To whom correspondence should be addressed.
E-mail: stayheavy@kangwon.ac.kr

into its acid form (HBEA) by heating it in air at 540℃ for six hours. Subsequently, we conducted ion exchange on the HBEA zeolites in an aqueous solution of $Co(NO_3)_2 \cdot 6H_2O$ (Sigma Aldrich, +98%) with stirring at room temperature for 24 hours [10]. The solids were separated from the solution, dried at 100℃, and then calcined at 550 ℃ under air for 4 hours. The weight percent of cobalt was estimated using inductively coupled plasma atomic emission spectroscopy (ICP-AES, Agilent 5900). The cobalt content is indicated in parentheses in the catalyst name (e.g., 'Co(0.57)HBEA' represents 0.57 wt.% cobalt ion-exchanged acid form BEA).

2-2. Characterization of catalyst

The BEA structure of fresh and aged catalysts was examined by X-ray diffraction (XRD) using a Miniflex instrument (Rigaku). The catalyst was mixed with 10 wt.% Ni powder (Sigma-Aldrich, < 150 μm, 99.99%) using an agar mortar for 30 minutes. The analysis was conducted in the 2 theta range of 4 to 50° at a scan rate of 0.001^o/min and an interval of 0.025^o, using Cu-Kα beam (λ = 1.5406 Å).

The atomic concentration of cobalt ion species on the surface was estimated by X-ray photoelectron spectroscopy (XPS) using a K-alpha instrument (Thermo Scientific). The analysis was performed under ultra-high vacuum conditions (5×10^{-9} mbar) with Al Kα X-ray as the beam source. The Co 2p XP spectra were calibrated by adjusting the C 1s peak at 284.8 eV.

2-3. Reaction test

The reaction tests were conducted using a fixed bed reactor system coupled with ozone production devices, as described in our previous publication [4]. Ozone was produced by flowing pure oxygen (5 ml/ min) through a wire-to-cylinder type dielectric barrier discharge (DBD) reactor powered by an AC power supply (Jungwoo System). The O_3-embedded O_2 flow was mixed with the flow of CH_4 (with or without H_2O and SO_2) balanced by N_2, just in front of the fixed catalyst bed. The typical gas composition included 500 ppm CH_4, $2,500 \pm 50$ ppm O_3, 10% O_2, 0, 2, or 3% H_2O, 0 or 1 ppm SO_2 and balanced by N_2. Total flow rate was 53 ml/min. The catalyst particle size was controlled within the range of 250–500 μm using standard sieves. We packed 80 mg of the sieved particles as a thin fixed bed over quartz wool layer in the middle of quartz tube. The reaction temperature was monitored and controlled at the center of the packed bed. The product flow emitted from the bed passed thorough an empty quartz tube reactor (the second reactor), whose inner temperature was maintained at 225℃ using a tubular furnace. This second reactor dissociated unreacted ozone slip without affecting the product composition. The product composition, excluding ozone, was analyzed by gas chromatography (Younglin Chromas, YL6500GC) equipped with a methanizer and flame ionization detector. Ozone concentration was monitored by a UV ozone meter (2B Technologies, 106M) before the product flow entered the second reactor. The amount of ozone used for methane conversion were calculated based on the concentrations of CO and CO_2 [4]. For detailed analysis conditions and specifications of the reaction units, refer to our previous paper [4].

3. Results and Discussions

Figure 1 presents the concentration of O_3 generated by DBD reactor. The power input to DBD reactor was controlled by changing the frequency of AC voltage from 100 to 700 Hz with the amplitude fixed at 14 kV. The power input increased from 0.6 to 6.6 W with the increase of AC frequency. For a feed flow of a pure O_2 (5 ml/min),
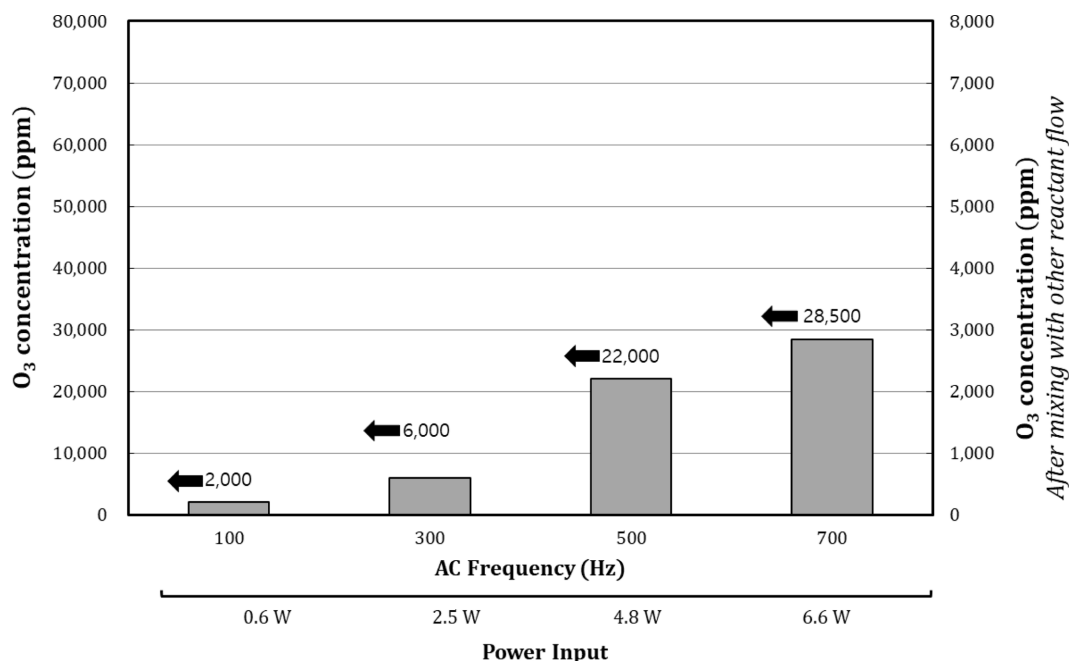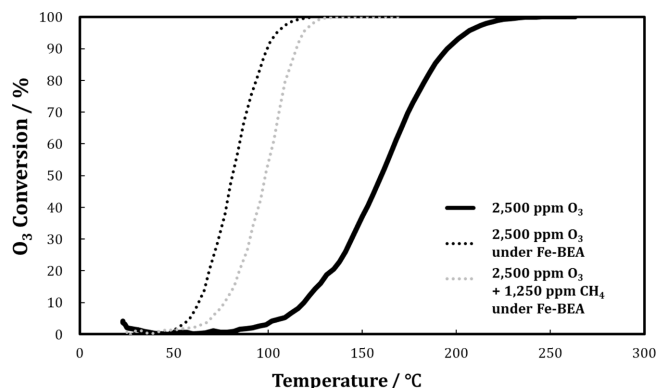

Fig. 1. The concentration of O_3 in the exit flow of DBD reactor: The feed = O_2 5 ml/min; The right y-axis is the O_3 concentration after mixing with CH_4/N_2 flow (48 ml/min).

Fig. 2. Decomposition of O_3 under temperature from 25 to 250 ℃: Feed gas = 2,500 ± 50 ppm O_3, 10% O_2 (with or without + 0.125% CH_4), N_2 balance ; Total flow rate = 53 ml/min: Catalyst = with or without Fe-BEA catalyst (Fe/Al = 0.05, Si/Al = 12.5, both in molar ratio).

the reactor emitted the flow containing 2,000~28,500 ppm O_3. It was diluted to 2,000~2,850 ppm by mixing with the other reactant flow (CH_4/N_2, 48 ml/min). The electric power required for generating ~25,000 ppm O_3 was about 5.6 W.

Ozone is a metastable gas species which decomposes into molecular oxygen when exposed to high temperatures. Figure 2 shows how ozone was converted into oxygen in the fixed bed reactor used for this study. As the temperature rises from room temperature, O_3 conversion gradually increases, reaching 100% conversion at around 250 ℃. Consequently, we anticipate that ozone will function as an oxidant at temperatures below 250 ℃, as it would otherwise undergo complete thermal decomposition. The decomposition of ozone was more enhanced in the presence of a zeolite catalyst (Fe-BEA). However, when a smaller amount of methane was included in the reactant, the decomposition was noticeably suppressed. This suggests that ozone and methane competitively adsorb onto the active sites of the zeolite
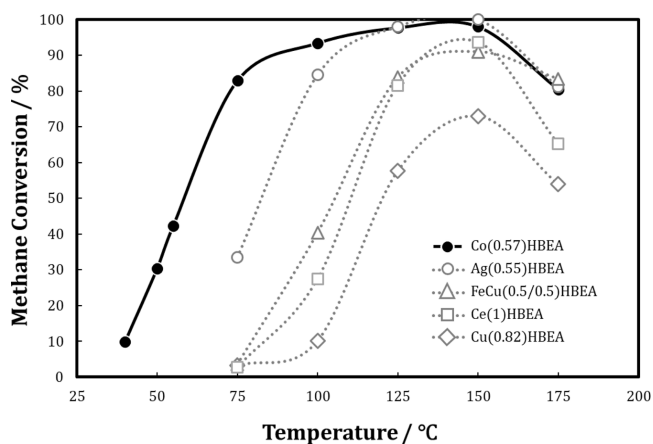

Fig. 3. Comparison of O_3-LMO activity of metal ion-exchanged BEA Catalysts: The figures in the parenthesis of catalyst names are the weight percent of the loaded metal; HBEA = proton form of BEA; Si/Al molar ratio of BEA = 12.5; Fixed bed = Catalyst 80 mg; Catalyst particle size = 250–500 μm; Feed gas = 500 ppm CH_4, 2,500 ± 50 ppm O_3, 10% O_2, and N_2 balance; Total flow rate = 53 ml/min.
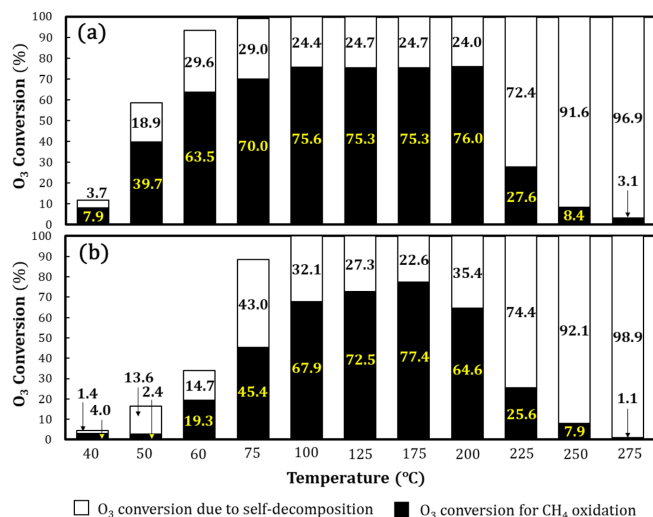
catalyst.

In our previous study, Co-BEA exhibited the highest activity among the transition metal-exchanged zeolite catalysts we investigated for lean methane oxidation by ozone [4]. In Figure 3, we compare Co-BEA with other transition metal-exchanged BEA catalysts in terms of O_3-LMO activity measured under dry reactant gas conditions. When using the Co(0.57)HBEA catalyst, CH_4 conversion exceeded 50% at approximately 60 ℃ and reached 100% at around 150 ℃. Notably, Co(0.57)HBEA showed significantly higher activity than other BEA catalysts in the low-temperature range below 150 ℃. However, CH_4 conversion gradually decreased as the temperature exceeded 150 ℃, which could be attributed to the accelerated thermal decomposition of ozone.

Then, the O_3-LMO activity of Co(0.57)HBEA was tested under wet reactant gases containing water vapor. The results were compared with the activity under dry reactant gas, as shown in Figures 4 and 5. The inclusion of water vapor led to the suppression of CH_4 conversion (Figure 4(a)). The decrease in catalytic activity was apparent at low temperatures (< 150 ℃). In contrast, the influence of water vapor was
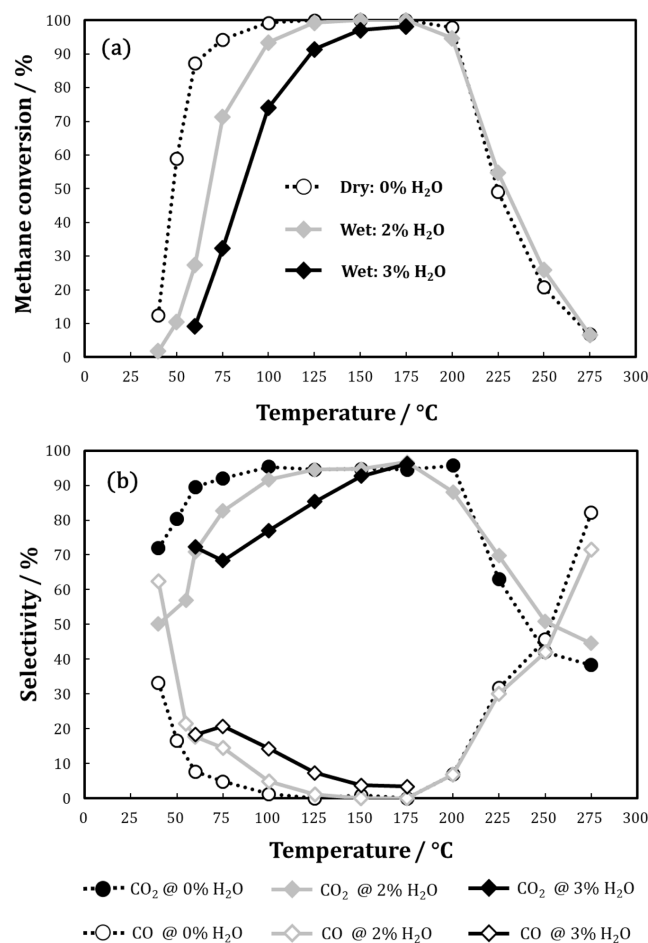
Fig. 4. The O_3-LMO activity of Co(0.57)HBEA under dry and wet conditions; (a) CH_4 conversions; (b) CO_2 and CO Selectivity; Fixed bed = Catalyst 80 mg; Catalyst particle size = 250–500 μm; Feed gas = 500 ppm CH_4, 2,500 ± 50 ppm O_3, 10% O_2, (0, 2, or 3%) H_2O, and N_2 balance; Total flow rate = 53.3 ml/min.
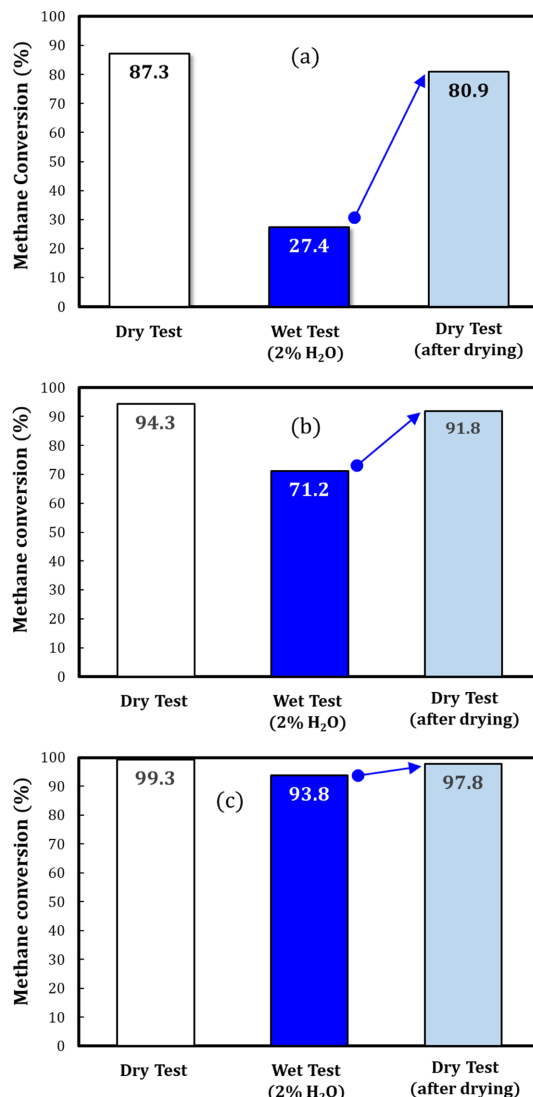
Fig. 5. O₃ conversion by the O₃-LMO catalysis of Co(0.57)HBEA: (a) under dry condition; (b) under wet condition (2% H₂O); Fixed bed = Catalyst 80 mg; Catalyst particle size = 250–500 μm; Feed gas = 500 ppm CH₄, 2,500 ± 50 ppm O₃, 10% O₂, (0, 2%) H₂O, and N₂ balance; Total flow rate = 53.3 ml/min.

insignificant at temperatures higher than 150℃. CO_2 selectivity was similarly affected by water vapor (Figure 4(b)). An increase in water vapor resulted in decreased CO_2 selectivity at temperatures below 150℃, but this influence was negligible at temperatures above 150℃. The side product observed was CO, and no other partial oxidation products were detected. Despite the presence of water vapor, steam methane reforming may not significantly contribute to CO production, as the reaction requires a high temperature of 800~1,000℃ [11].

Figure 5 illustrates the efficiency of Co(0.57)HBEA in utilizing O_3 as an oxidant for CH_4 oxidation. Co(0.57)HBEA enhanced O_3 conversion, lowering the complete conversion temperature from 250 to 75℃ under dry conditions. Co(0.57)HBEA utilizes over 70% of converted O_3 for CH_4 oxidation to carbon oxides at 50~200℃. The O_3 conversion was comparatively suppressed under wet conditions, raising complete conversion temperature to 100℃. However, the O_3 utilization efficiency for CH_4 conversion remained largely unaffected.

The Co(0.57)HBEA catalyst, tested under wet conditions (2% H₂O), underwent vacuum drying at 250℃ and 10 mmHg. Subsequently, its activity was evaluated under dry conditions. In Figure 6, the third bars of the three graphs represent the dry-test activity of the vacuum-dried catalyst. Notably, the vacuum-dried catalyst regained most of its initial dry-test activity at 60, 75 and 100℃, suggesting that the reduction in activity under wet conditions was not due to chemical deactivation. It is hypothesized that water vapor physically adsorbed onto the catalyst, inhibiting the adsorption of methane and ozone. In the prolonged reaction test (Figure 7), the catalyst maintained its activity under wet condition (3% H₂O) for 18 hours, which supports there is no activity loss due to structural degradation.

We investigated how the O₃-LMO activity of Co(0.57)HBEA would change if the catalyst were aged under harsh hydrothermal conditions. The fresh Co(0.57)HBEA was hydrothermally aged for

Fig. 6. CH₄ conversion by Co(0.57)HBEA under dry and wet (2% H₂O) conditions at (a) 60, (b) 75 and (c) 100℃. The third bar in each graph is the dry-test activity of Co(0.57)HBEA which was vacuum dried (250℃, 10 mmHg) after having been tested under wet (2% H₂O) conditions; The reaction conditions were the same as in Figure 5.
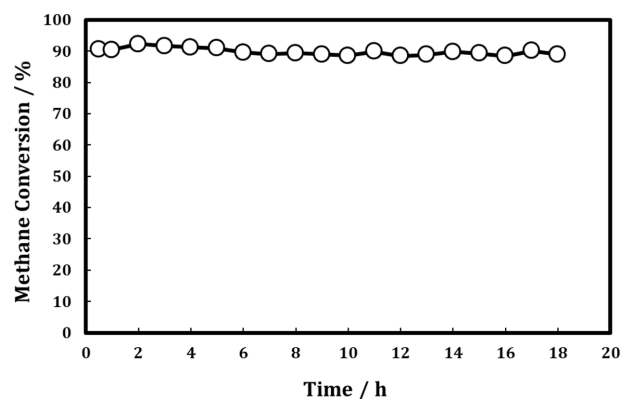
Fig. 7. The prolonged reaction test of Co(0.57)HBEA under wet condition at 125℃; Fixed bed = Catalyst 80 mg; Catalyst particle size = 250–500 μm; Feed gas = 500 ppm CH₄, 2,500 ± 50 ppm O₂, 10% O₂, 3% H₂O, and N₂ balance; Total flow rate = 53.3 ml/min.
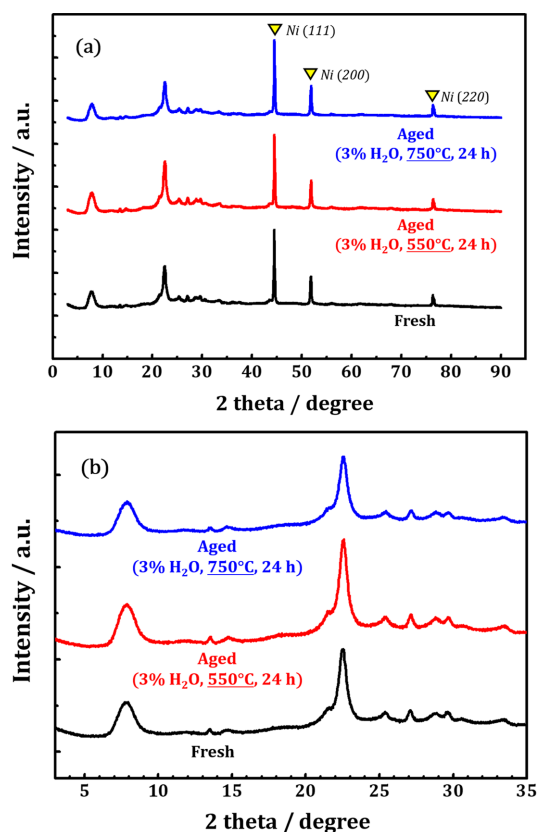
Fig. 8. XRD spectra of the fresh and hydrothermally aged Co(0.57) HBEAs; (a) Wide angle spectrum including internal standard Ni peaks; (b) Narrow angle spectrum excluding internal standard peaks.
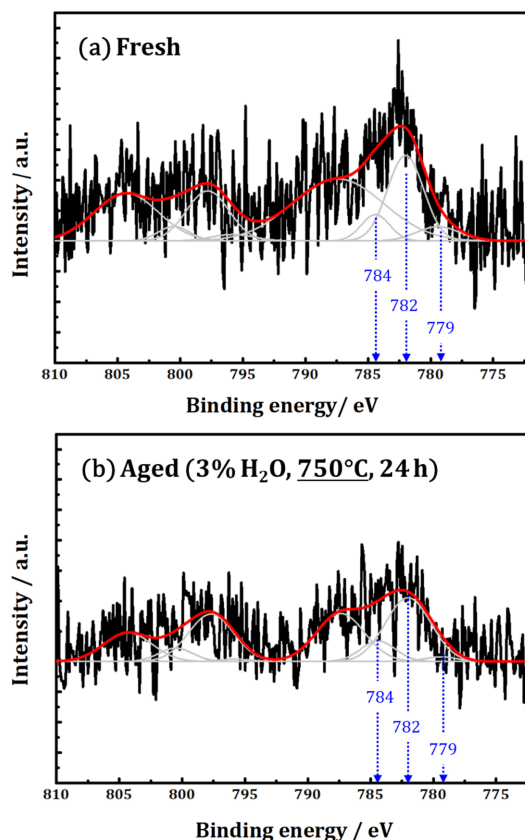

Fig. 9. Co 2p XPS spectra of the fresh and hydrothermally aged catalysts; (a) Fresh Co(0.57)HBEA; (b) Hydrothermally aged Co(0.57)HBEA at 750℃ for 24 hours with flowing the reactant gas containing 3% H_2O (Gas composition: 500 ppm CH_4, $2,500 \pm 50$ ppm O_3, 10% O_2, 3% H_2O, and N_2 balance; Total flow rate = 53.3 ml/min); The core-level binding energies were corrected by adjusting the C 1s peak position at 284.8 eV.

24 hours at 550 and 750℃ in the presence of a reactant gas containing 3% H_2O. The aged catalysts were vacuum-dried before performing analysis and reaction tests. Figure 8 shows the XRD spectra of the aged catalysts were similar to that of the fresh catalyst, implying that the BEA structure was almost intact under hydrothermal treatments. However, the Co 2p XPS analysis (Figure 9 and Table 1) revealed the number of active cobalt species on the surface reduced after hydrothermal aging at 750℃. The peak areas of mono and polynuclear Co^{2+} species, which are known to be redox-active in methane oxidation [4], decreased by 30% after hydrothermal aging at 750℃ (Table 1). Overall, the Co 2p peak area decreased noticeably after the aging (Figure 9), suggesting the surface cobalt species agglomerated under hydrothermal treatment at 750℃. The O_3-LMO activity of the aged catalysts were then examined. Figure 10 shows that CH_4 conversions decreased at the reaction temperatures over 175℃ as the hydrothermal aging temperature increased. This result suggests structural deformation of the catalyst, such as active metal agglomeration, contributes to the decline in O_3-LMO activity. However, O_3-LMO is fundamentally
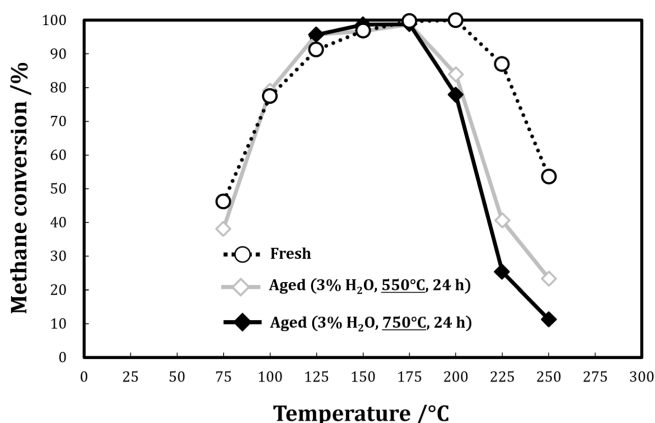

Fig. 10. The O_3-LMO activities of the fresh and hydrothermally aged Co(0.57)HBEAs under wet condition; Fixed bed = Catalyst 80 mg; Catalyst particle size = 250–500 μm; Feed gas = 500 ppm CH_4, $2,500 \pm 50$ ppm O_3, 10% O_2, 3% H_2O, and N_2 balance; Total flow rate = 53.3 ml/min.

Table 1. The Co 2p XPS peak areas of Co(III) and Co(II) species in the fresh and hydrothermally aged Co(0.57)HBEA: The areas were calculated from the deconvolution results in Figure 9

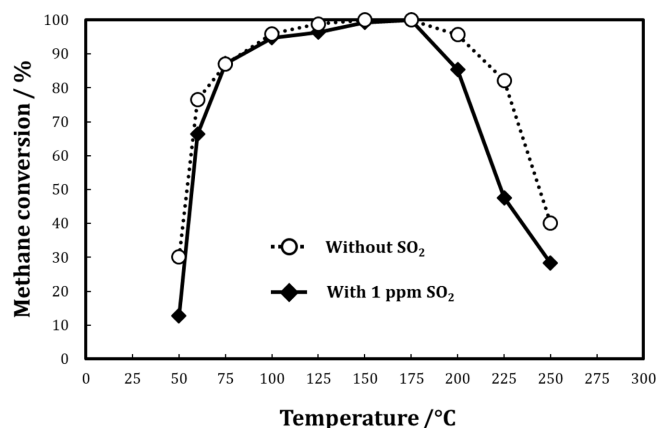| Catalyst ▼	Co(III) polynuclear (779 eV)	Co(II) mononuclear (782 eV)	Co(II) polynuclear (784 eV)	Area Sum
Fresh	720.2	3653.6	883.2	5257.0
Aged (3% H_2O, 750℃, 24 h)	133.1	2558.7	635.5	3327.4

Fig. 11. The effect of sulfur oxide on the O_3-LMO activity of Co(0.57) HBEA under a dry condition; Fixed bed = Catalyst 80 mg; Catalyst particle size = 250–500 μm; Feed gas = 500 ppm CH_4, $2,500 \pm 50$ ppm O_3, 10% O_2, 0 or 1 ppm SO_2, and N_2 balance; Total flow rate = 53.3 ml/min.

unsuitable for temperatures that induce structural deformation in the Co-BEA catalyst, as ozone undergoes complete thermal decomposition at such high temperatures.

In our final investigation, we examined the influence of sulfur poisoning on the O_3-LMO activity of Co(0.57)HBEA. Despite its low concentration, sulfur compounds are consistently present in the lean methane emission sources, such as natural gas engine exhausts [12,13], landfill gas [14,15], and livestock emissions [16]. Sulfur tolerance is always a significant issue for Co-BEA catalysts used in industrial applications [17,18]. Specifically, sulfur species like sulfur dioxide (SO_2) interact with the active sites, leading to the formation of stable cobalt-sulfate species. These sulfates obstruct the active sites, significantly reducing the redox activity of Co-BEAs [18]. We observed a similar poisoning effect in the O_3-LMO catalysis of Co(0.57)HBEA (Figure 11). As SO_2 was added to the reactant gas, methane conversion was depressed, despite the low concentration of SO_2 (approximately 1 ppm).

In summary, the 'Co-BEA-based O_3-LMO system' effectively oxidizes lean methane emissions at low temperatures, preferably within the range of 100 to 200℃. The water vapor in the reactant gas does not deactivate the system, but thorough desulfurization of the reactant is mandatory for the viable application of this strategy.

4. Conclusions

The ozone oxidation of lean methane was effectively facilitated by the cobalt-exchanged BEA catalyst, Co(0.57)HBEA. This catalyst exhibited CH_4 conversions exceeding 70% within the temperature range of 100~200℃, even under wet conditions containing 2 or 3% H_2O. Water vapor reduced CH_4 conversion and CO_2 selectivity, but this effect was insignificant at temperatures higher than 150℃. The O_3 utilization efficiency for CH_4 conversion remained largely unaffected by water vapor. The decreased activity of Co(0.57)HBEA due to

exposure to water vapor at 60~100℃ could be easily restored through vacuum drying of the wet catalyst. No evidence of catalyst deactivation caused by water vapor was observed, and the catalyst maintained consistent activity for 18 hours in prolonged reaction tests at 100℃ under a wet condition (3% H_2O). While the influence of water vapor existed, it was not severe unless the temperature was high enough to cause hydrothermal deactivation, such as active metal agglomeration. However, sulfur oxide (SO_2) in the reactant gas adversely affected the O_3-LMO activity of Co(0.57)HBEA, likely due to the formation of stable cobalt-sulfate species.

References

1. https://www.epa.gov/ghgemissions/understanding-global-warming-potentials.
2. Jackson, R. B., Solomon, E. I., Canadell, J. G., Cargnello M. and Field, C. B., "Methane Removal and Atmospheric Restoration," *Nat. Sustain*., **2**(6), 436-438(2019).
3. Etminan, M., Myhre, G., Highwood, E. J. and Shine, K. P., "Radiative Forcing of Carbon Dioxide, Methane, and Nitrous Oxide: A Significant Revision of the Methane Radiative Forcing," *Geophys. Res. Lett*., **43**, 12614-12623(2016).
4. Jin, S. M., Lee, K.-Y. and Lee, D.-W., "Ozone-Induced Lean Methane Oxidation over Cobalt Ion-Exchanged BEA Catalyst under Dry Reaction Conditions," *J. Ind. Eng. Chem*., **112**, 296-306(2022).
5. Lee, S. W., Kim, E. J., Lee H. J. and Park, J. H., "Preparation of the Hollow Fiber Type Perovskite Catalyst for Methane Complete Oxidation," *Korean Chem. Eng. Res*., **56**(3), 297-302(2018).
6. Kim, S., Lee, J. Y., Cho, I., Lee, D.-W. and Lee, K.-Y., "Catalytic Combustion of Methane over $AMnAl_{11}O_{19}$(A=La, Sr, Ba) and $CeO_2/LaMnAl_{11}O_{19}$," *Korean Chem. Eng. Res*., **49**(5), 633-638(2011).
7. Hui, K. S., Kwong, C. W. and Chao, C. Y. H., "Methane Emission Abatement by Pd-ion-exchanged zeolite 13X with Ozone," *Energy. Environ. Sci*., **3**, 1092-1098(2010).
8. Keenan, M., Nicole, J. and Poojary, D., "Ozone as an Enabler for Low Temperature Methane Control over a Current Production Fe-BEA Catalyst," *Top. Catal*., **62**, 351-355(2019).
9. Yasumura, S., Saita, K., Miyakage, T., Nagai, K., Kon, K., Toyao, T., Maeno, Z., Taketsugu, T. and Shimizu, K., "Designing Maingroup Catalysts for Low-temperature Methane Combustion by Ozone," *Nat. Commun*., **14**, 3926:1-10(2023).
10. Beznis, N. V., Weckhuysen, B. M. and Bitter J. H., "Partial Oxidation of Methane Over Co-ZSM-5: Tuning the Oxygenate Selectivity by Altering the Preparation Route," *Catal. Lett*., **136**, 52-56(2010).
11. Torimoto, M., Ogo, S., Hisai, Y., Nakano, N., Takahashi, A., Ma, Q., Seo, J. G., Tsuneki, H., Norby, T. and Sekine, Y., "Support Effects on Catalysis of Low Temperature Methane Steam Reforming," *RSC Adv*., **10**, 26418-26424(2020).
12. Lott, P. and Deutschmann, O., "Lean-Burn Natural Gas Engines: Challenges and Concepts for an Efficient Exhaust Gas Aftertreatment System," *Emiss. Control Sci. Technol*., **7**, 1-6(2021).
13. Kinnunen, N., Kinnunen, T. and Kallinen, K., "Improved Sulfur Resistance of Noble Metal Catalyst for Lean-Burn Natural Gas

Applications," *SAE Tech.* Paper 2013-24-0155 (2013).

14. Ungary, C., "A Sustainable Approach to the Conversion of Waste into Energy: Landfill Gas-to-Fuel Technology," *Sustainability*, **15**(20), 14782:1-17(2023).

15. Manheim, D. C., Yeşiller, N. J. and Hanson, L., "Gas Emissions from Municipal Solid Waste Landfills: A Comprehensive Review and Analysis of Global Data," *J. Indian Inst. Sci.*, **101**, 625-657 (2021).

16. Feilberg, A., Hansen, M. J., Liu, D. and Nyord, T., "Contribution of Livestock H_2S to Total Sulfur Emissions in a Region with Intensive Animal Production," *Nat. Commun.*, **1069**, 1-7(2017).

17. Kumar, S. N., Appari, S. and Kuncharam B. V. R., "Techniques for Overcoming Sulfur Poisoning of Catalyst Employed in Hydrocarbon Reforming," *Catal. Surv. Asia*, **25**, 362-388(2021).

18. Luo, J., Xu, H., Liang, X., Wu, S., Liu, Z., Tie, Y., Li, M. and Yang, D., "Research Progress on Selective Catalytic Reduction of NOx by NH_3 over Copper Zeolite Catalysts at Low Temperature: Reaction Mechanism and Catalyst Deactivation," *Res. Chem. Intermed.*, **49**, 2321-2357(2023).

Authors

So Min Jin: PhD Candidate, Department of Chemical Engineering, Kangwon National University, Gangwon-do, 24341, Korea; jinssol11@kangwon.ac.kr

Dae-Won Lee: Professor, Department of Chemical Engineering, Kangwon National University, Gangwon-do, 24341, Korea; stayheavy@kangwon.ac.kr